Journal of Alloys and Compounds 505 (2010) 337–342

Contents lists available at ScienceDirect

Journal of Alloys and Compounds

journal homepage: www.elsevier.com/locate/jallcom

Nickel assisted sintering of Ti_3SiC_2 powder under pressureless conditions

Bharat Bhooshan Panigrahi[a,*], N. Subba Reddy[b], Avinash Balakrishnan[c], Min-Cheol Chu[d], Seong-Jai Cho[d], Jose J. Gracio[a]

[a] Center for Mechanical Technology and Automation, Department of Mechanical Engineering, University of Aveiro, Aveiro 3810-193, Portugal
[b] Division of Materials Science and Engineering, Engineering Research Center, Gyeongsang National University, Chinju 660-701, Republic of Korea
[c] SIMAP, CNRS, Groupe GPM2, Grenoble-INP, 38402 Saint Martin d'Heres Cedex, France
[d] Division of Advanced Technology, Korea Research Institute of Standards and Science, Yuseong, Daejeon 305-340, Republic of Korea

ARTICLE INFO

Article history:
Received 11 November 2009
Received in revised form 12 May 2010
Accepted 25 May 2010
Available online 18 June 2010

Keywords:
Cold-isostatic pressing
Sintering
Activation energy
Mechanical properties

ABSTRACT

This investigation was aimed to study the effect of nickel addition on the sintering behaviour of Ti_3SiC_2 powder under pressureless conditions. Nearly pure bulk Ti_3SiC_2 ceramic with relative density of ~98.5% was produced at 1500 °C by sintering of Ti_3SiC_2 powder while using 1 wt.% nickel as a sintering aid. The activation energy of sintering of Ti_3SiC_2 powder was determined to be 351 ± 5 kJ/mol, which was decreased slightly to 305 ± 10 kJ/mol when nickel (1 wt.%) was added. Sintering of Ti_3SiC_2 powder was found to be controlled by mixed mode of mechanisms, i.e., the interface reactions and diffusion of Si atoms. The mechanism was changed to liquid phase sintering due to melting of Ni-based compounds in the sample sintered with Ni. The reaction of Ni with Ti_3SiC_2 helped to decrease the grain growth rate. The hardness (Vickers), flexural strength and fracture toughness of the sintered Ti_3SiC_2–1Ni sample were found to be 3.4 GPa, 311 ± 22 MPa and 2.8–6.4 MPa $m^{1/2}$, respectively.

1. Introduction

In recent times, the ternary carbides with hexagonal structure, known as MAX phases, have taken a considerable attention from structural ceramists [1,2]. With a good high temperature strength, corrosion resistant, oxidation resistant, good tribological properties, elastic stiffness, good thermal and electrical properties, they exhibit an excellent machinability. Ti_3SiC_2 (TSC) is the most widely studied compound in this group which is produced using various combinations of raw materials [3–6] including Ti, Si, C, TiC and SiC. To enhance the purity of TSC phase, excess amount of Si, small amounts of Al and B_2O_3 powders were used [7–9] and the high purity TSC powder was produced from Ti, Si and TiC powders using 0.10–1.0 mol of extra Si [10–12]. The high density parts of TSC were produced through hot pressing, pulse discharge sintering, spark plasma sintering and self propagating high temperature synthesis processes [3,13–17]. There are some reports on synthesis of TSC by pressureless sintering using Al [18–21] and B_2O_3 [7] as sintering aids and sintering the ball milled ultra fine powders [22]; however, the final density of over 90% could not be achieved. Pressureless sintering of MAX phase powder is difficult due to its easy decomposability at high temperatures, i.e., often subjected to the loss of Si from TSC or Al from Ti_3AlC_2 and Cr_2AlC powders. Another important issue during sintering of these compounds is not only the processing atmosphere (i.e., vacuum or inert atmosphere), but the type of furnace used, i.e., graphite heating or non-graphite heating furnaces. High density body was produced by pressing the powder cold-isostatically at a very high pressure of about 380 MPa, followed by the pressureless sintering [23]. A mechanically alloyed powder with about 80 vol.% TSC [24] and the preform prepared by tape casting of TSC powder (~95 vol.% purity) were sintered to nearly full density [25]. Since the sample was sintered on a graphite heating furnace, the effect of carbon diffusion from atmosphere into the sample was noticed; consequently the titanium carbide content in the sintered body was increased significantly. To reduce the amount of TiC_x, large amount (about 10 wt.%) of Si powder was mixed with TSC powder during sintering [25]. Recently, TSC powder with small amounts (1 and 2 wt.%) of Si was sintered under pressureless condition on a tungsten heating furnace [26]; the final product had a very low amount of impurities. However, there is no reported study on the sintering kinetic of TSC powder so far.

Nickel was used as a sintering aid for the metal and the ceramic powders. Nickel is known as a fast diffuser in the metal, such as titanium, and was found to enhance the sintering rates of titanium [27], tungsten [28] and some ceramic powders [29]. It was also observed that nickel suppressed the grain coarsening process up to some extent during sintering [27]. It would be worth investigating if sintering of TSC powder could be enhanced by nickel addition. The present investigation has been initiated with an aim to produce high purity dense body of TSC powder by sintering under

* Corresponding author. Tel.: +351 234 370830x23887; fax: +351 234 370953.
E-mail addresses: bharat@ua.pt, panigrahi14@yahoo.com (B.B. Panigrahi).

0925-8388/$ – see front matter © 2010 Elsevier B.V. All rights reserved.
doi:10.1016/j.jallcom.2010.05.177

pressureless conditions using small amount of nickel as a sintering aid. Attempts have been made to study the sintering kinetics of TSC powder and to evaluate the mechanical properties of the sintered body.

2. Experimental

TSC powder was produced using $TiC_{x(x=0.67)}$ and Si powders as reported earlier [26]. The TiC_x and Si powders were mixed in a molar ratio of 3:1 and pressed using 20 mm cylindrical steel die at a uniaxial pressure of about 20 MPa. The compact was heated to a temperature of 1150 °C for 2 h under high purity argon. The cooled sample was ground with the help of an agate mortar-pastel and the particles sieved using −400 mesh screens were collected as final TSC powder. The synthesized powder contains ~96 wt.% Ti_3SiC_2, ~3.5 wt.% TiC and ~0.5 wt.% of $TiSi_2$ and Ti_5Si_3C phases [26]. The particle size was analyzed using Helos particle size analyzer (Sympatec GmbH, Germany).

Two types of powders were taken for sintering: (a) TSC powder, and (b) mixed powders of TSC + 1 wt.% Ni (designated as TSC–1Ni). About 4 wt.% of binder (paraffin wax) was first dissolved in toluene and then the powders (either TSC or TSC–1Ni) were mixed by ball milling for about 1 h (at 100 rpm) and dried. Powders were compacted in a steel die (diameter of ~10 mm) uniaxially, initially at a very low pressure (~10 MPa) and then cold iso-statically pressed (CIP, Kovaco, Incheon, Korea) at a pressure of 275 MPa for a holding time of 1 min. The relative densities of green compacts were around 68%. The green compact was kept in the alumina crucible and placed into the tungsten heating furnace. After charging the sample, the furnace chamber was evacuated to a vacuum level of 10^{-2} bar and subsequently flushed-out by high purity argon for 30 min. The furnace was heated at a rate of 5 °C min^{-1} and held at 200 °C for 20 min under vacuum (10^{-2} bar), to remove the binder effectively. Next, the furnace was heated at a rate of 10 °C min^{-1} up to the final sintering temperature ranging from 1300 to 1600 °C for the isothermal periods of 1 and 4 h under flowing argon. To determine the onset temperature of sintering, green compacts of TSC and TSC–1Ni samples were sintered on a dilatometer system (DIL 402C, Netzsch-Geratebau GmbH, Germany), while heating at a constant rate of 10 °C/min up to 1200 °C (the maximum operating temperature of the system). Samples were characterised using X-ray diffraction (XRD, Rigaku Co., Japan) using Cu λ = 1.54056 Å radiation with a step size of $2\theta = 0.01°$ and using scanning electron microscope (SEM, Akashi Co., Japan). Prior to the SEM examination, the polished samples were etched with HF–HNO_3–H_2O solution (mixed in a volume ratio of 1:1:2). The hardness, flexural strength and fracture toughness (*R*-curve behaviour) of sintered samples were measured.

3. Results and discussion

3.1. Material characterization and sintering

The XRD patterns of the synthesized powders (Fig. 1) show that Ti_3SiC_2 is a major phase and TiC_x is the only other phase. The peak corresponds to $TiSi_2$ was not detected due to very low amount. The particle size analysis of the powder shows (Fig. 2) a peak around 15 μm and the particles have been distributed over a wide range. The SEM micrograph of TSC powder shows (Fig. 3) the particles are irregular shaped and having stepped structures as revealed by a high resolution image (Fig. 3 in-set). During XRD analysis (Fig. 1), the TSC samples sintered at 1400 and 1500 °C show extremely small or no peaks of TiC phase. This could be attributed to the conversion of residual impurities on the powder during sintering (the reaction is: $9TiC + Ti_5Si_3C + TiSi_2 = 5Ti_3SiC_2$). At 1600 °C the peaks of TiC_x phase were emerged once again. Like TSC sample, TSC–1Ni sample also exhibited high purity level at 1500 °C (sintered for 1 h), i.e., peaks of only Ti_3SiC_2 were visible and when the sample was sintered for longer time (for 4 h) at 1500 °C, small peak of Ni_3Si_2 and very faint peaks of Ni–Si–Ti ternary compounds were found. When TSC–1Ni sample was sintered at 1600 °C, the peak of Ni_3Si_2 disappeared while peaks of TiC_x emerged once again, with relatively increased intensity (compared to that of the TSC sample) and some faint peaks of Ni–Si–Ti ternary compounds were also detected (Fig. 1). The quantitative analysis of TiC phase content on the sample sintered at 1600 °C was carried out from the XRD patterns (using method reported in literature [26]) while assuming two phases (TSC and TiC) mixture. The amount of TiC was found to be ~4 wt.% in TSC sample, whereas in the TSC–1Ni sample, it increased significantly to ~17 wt.%, at 1600 °C.

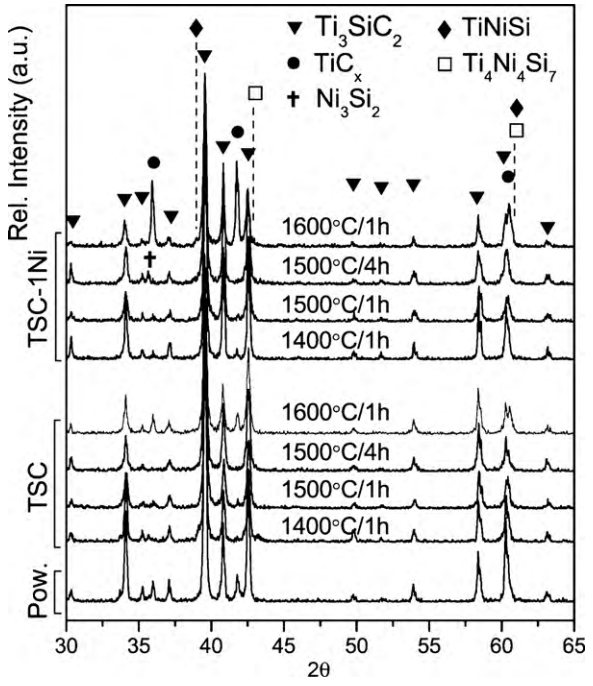

Fig. 1. XRD patterns of TSC powder and the sintered samples of TSC and TSC–1Ni at various conditions.

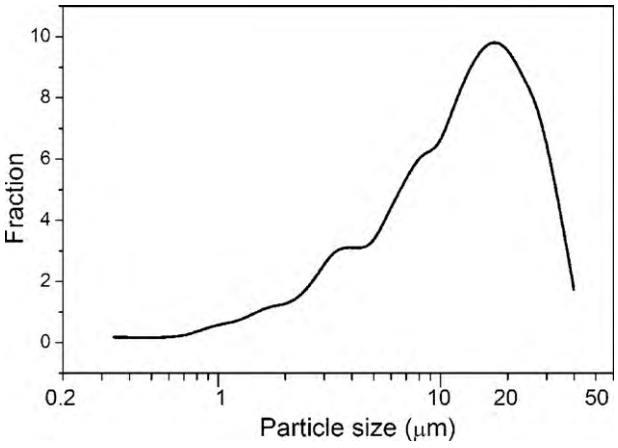

Fig. 2. Particle size analysis of TSC powder.

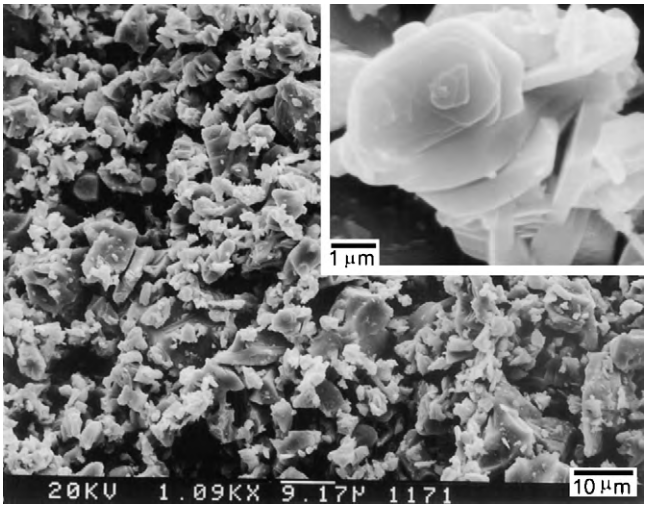

Fig. 3. SEM micrograph of TSC powder. High resolution image (in-set) of one particle showing the layered structure.

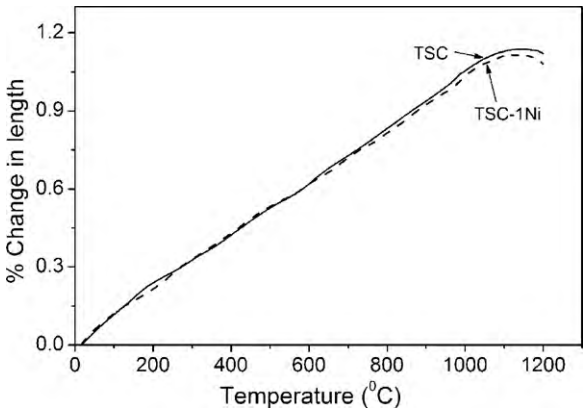

Fig. 4. Dilatometric curves of the green compacts of TSC and TSC–1Ni samples, heated at a rate of 10 °C/min.

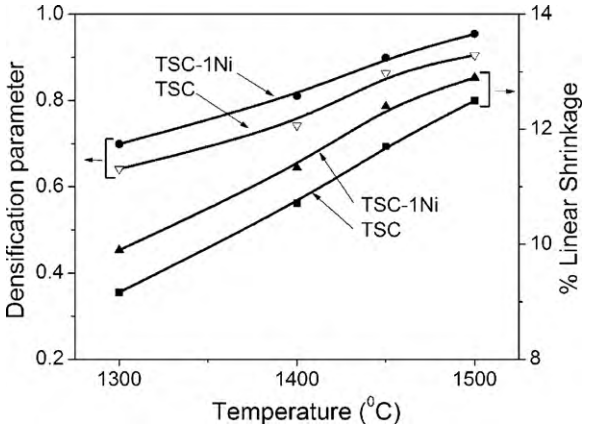

Fig. 6. Densification parameters and measured linear shrinkages at various temperatures.

The dilatometric plot of TSC compact shows (Fig. 4) that the sample expanded almost linearly up to about 1060 °C. The coefficient of thermal expansion of the green compact (which has a green density of about 68%) was estimated to be 10.9×10^{-6} °C^{-1} which is close to the values reported [5] for TSC. At around 1060 °C the expansion tends to decrease and it was stopped completely at around 1140 °C, followed by a shrinkage. There was no significant difference in the nature of dilatometric curve obtained for TSC–1Ni.

The densities of the sintered samples increased almost linearly up to 1500 °C (Fig. 5) and slowly up to 1600 °C. To estimate the relative density of sintered body, the composition of the sample was determined for the phases detected during XRD analysis. Since the TSC samples, sintered up to 1500 °C show TSC as a major phase, the theoretical density of TSC (4.512 g/cm^3) was taken as a reference while ignoring the presence of TiC phase due to its low amount. For TSC samples sintered at 1600 °C, which contains 4 wt.% of TiC, the theoretical density was calculated for a mixture of 96 wt.% TSC and 4 wt.% TiC. In case of TSC–1Ni samples, along with TiC, Ni based compounds were also present, but quantitative estimation could not be made due very small amounts. Therefore, to estimate the relative density, theoretical density was calculated for a mixture of 99 wt.% TSC and 1 wt.% Ni up to 1500 °C, for a approximation. For TSC–1Ni sample sintered at 1600 °C, where TiC phase content was 17 wt.%, the theoretical density was calculated for a mixture of 82 wt.% TSC, 17 wt.% TiC and 1 wt.% Ni while ignoring the amount of Ni based binary and ternary compounds. The relative densities of TSC samples were reached to about 96% and 98% after sintering at 1500 and 1600 °C, respectively (Fig. 5). When the sample was sintered for longer time (4 h) at 1500 °C the TSC sample could reach to a density of 98% (Fig. 5 inset). During sintering (Fig. 5) the density of about 98.5% was obtained at 1500 °C for holding time of 1 h and there was no further improvement in the density of TSC–1Ni sample when sintered for 4 h at 1500 °C. The relative density decreased slightly when TSC–1Ni sample sintered at 1600 °C, which could be attributed to the decomposition of TSC phase. The densification parameters [$(\rho_s - \rho_0)/(\rho_{th} - \rho_0)$, where ρ_0, ρ_s, and ρ_{th} are the green, sintered and theoretical densities respectively] of the samples have been shown in Fig. 6. The Ni added sample shows relatively larger values of densification parameter. The measured linear shrinkage ($\Delta L/L$, where ΔL is the decrease in the initial length L) shows (Fig. 6) that TSC sample shrank by about 12.5% whereas TSC–1Ni sample shrank by nearly 13% at 1500 °C (after 1 h of sintering).

The SEM micrograph of TSC sample sintered at 1500 °C (for 1 h) shows (Fig. 7) the bimodal nature of the microstructure, i.e., consists of large grains and very fine grains of TSC phase, which could be attributed to the bimodal distribution of the initial particles in the powder (Fig. 3). When the TSC sample was sintered for 4 h at 1500 °C, the fine grains disappeared and relatively large and

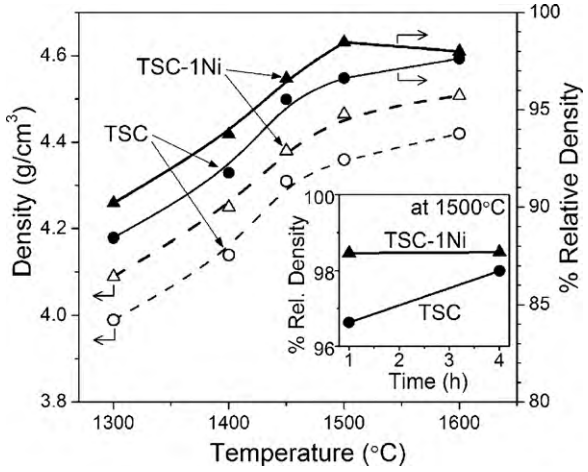

Fig. 5. Variation of true density and relative density of samples as a function of temperature. Relative density as a function of holding time has been shown in the inset.

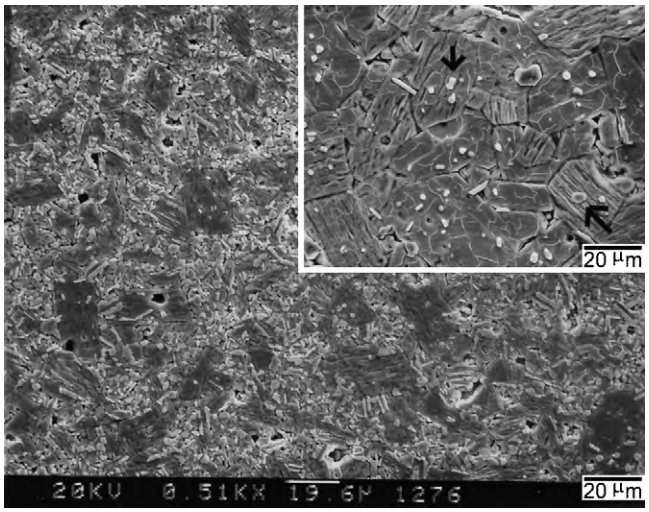

Fig. 7. SEM micrograph of TSC sample sintered at 1500 °C for 1 h and the sample sintered for 4 h has been shown in in-set. TiC grains have been marked by the arrows.

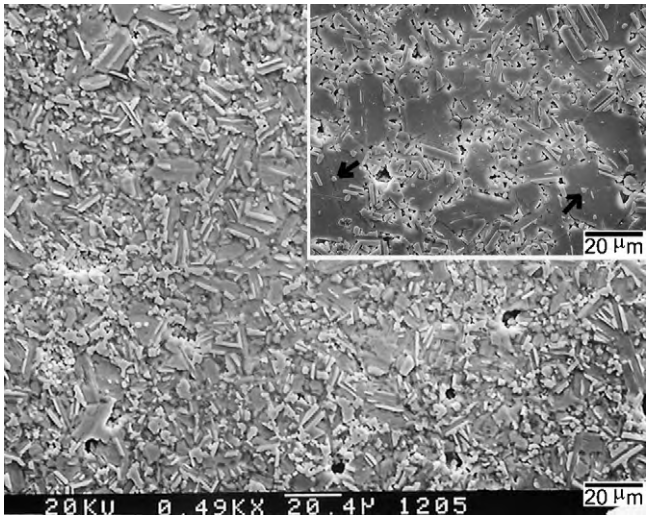

Fig. 8. SEM micrograph of TSC–1Ni sample sintered at 1500 °C for 1 h and the sample sintered for 4 h has been shown in in-set. TiC grains have been marked by the arrows.

uniformly distributed grains of pure TSC were observed (in-set in Fig. 7). The microstructures of TSC–1Ni sample shows (Fig. 8) the number of fine grains is relatively more compared to that of TSC samples. Unlike TSC sample, the fine grains in the TSC–1Ni sample did not disappear after sintering for 4 h at 1500 °C, although the relative number of fine grains was declined (compared to the sample sintered for 1 h) and the number of large grains was increased (in-set of Fig. 8). Ni is known to form a large number of binary and ternary compounds with Si and Ti; during sintering of TSC–1Ni sample, Ni reacts with TSC and tends to decompose it to form binary and ternary compounds. Since, many of Ni based compounds have low melting point than the present sintering temperature, some amount of liquid is formed which helps in sintering of TSC–1Ni sample. However, the formation of Ni based compound, appears to be very low up to 1500 °C (1 h) and produces high purity TSC sample at this condition. The attempt to decompose TSC phase by Ni, causes decrease in the grain growth rate of TSC, hence significantly large number of fine grains are present in TSC–1Ni sample (Fig. 8) compared to that of TSC sample (Fig. 7). Small grains of TiC were also seen in the microstructures with a very bright colour (shown in Figs. 7 and 8) and some of the grains of TiC are embedded within the TSC phase, as reported by other investigators [30,31] also.

3.2. Analysis of sintering kinetics

Attempts have been made to understand the sintering kinetics of TSC powder by estimating the activation energies (AE) of sintering using the linear shrinkage data (shown in Fig. 6). The AE of sintering (Q) was obtained from the following relation [32]:

$$\ln \frac{\Delta L}{L} = C - \frac{nQ}{RT} + n \ln t \quad (1)$$

where T is the temperature, t is the time, n is a sintering time factor, R is the universal gas constant and C is a constant. The value of n was obtained from slope of the logarithmic plots of shrinkage and time, as shown in Fig. 9 and it was found to yield very low and similar values (0.1) for both, TSC and TSC–1Ni. Fig. 10 shows the Arrhenius plot of the shrinkage versus inverse of temperatures for both the samples. The value of Q for TSC powder was found to be 351 ± 5 kJ/mol and decreased slightly to 305 ± 10 kJ/mol when nickel was added. To understand the significance of measured Q values in the present investigation, the results were compared with the AEs of diffusions reported in the literature. Ideally, the data should

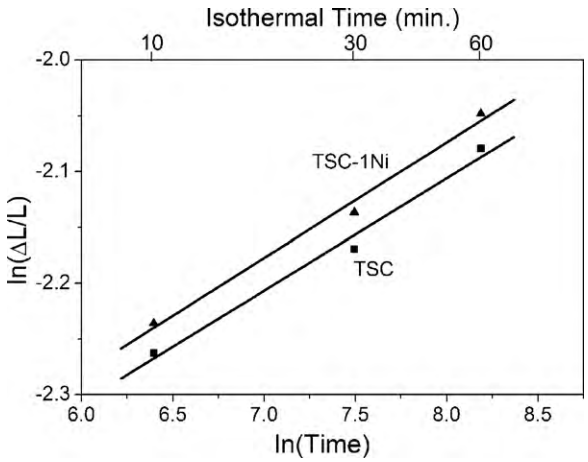

Fig. 9. The log–log plots of linear shrinkage and isothermal time (for the sample sintered at 1500 °C), to determine the value of n.

be compared with the diffusion properties of the Ti–Si–C ternary system; however, diffusion studies on Ti–Si–C ternary system are not available at this moment. Data have been therefore compared with the diffusion properties of Ti–Si, Si–C and Ti–C binary systems (shown in Table A.1). Unfortunately, the measure Q values in present work, do not match with any of the AEs of the diffusions of binary systems, shown in appendix.

It was earlier [26] pointed out that sintering of TSC powder was partially contributed by the reaction of impurities of TiC_x and tita-

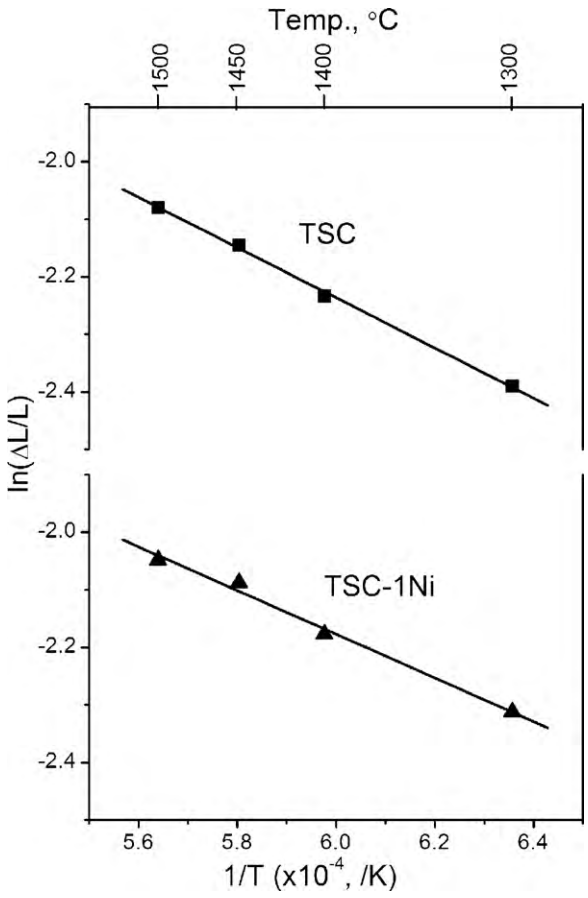

Fig. 10. Arrhenius plots of the linear shrinkage data with respect to the inverse of temperature, to determine the value of Q.

nium silicides to form TSC, hence the purity as well as density was increased with increasing temperature. In the Ti_3SiC_2 system, Si–Ti bond is regarded as a weakest link in the system and hence Si atom is more prone to diffuse and escape during the sintering. It appears that Si diffusion played a dominating role during sintering of TSC powder. When TSC–1Ni sample was sintered at 1500 °C, a number of processes occurred concurrently, such as: (a) reaction of retained impurities of powder, (b) reaction of Ni with Si and Ti of TSC to form binary and ternary compounds, and (c) formation of Ni based liquid phase. Thus the sintering rate was increased on TSC–1Ni sample. Although the peaks (Fig. 1) corresponding to Ni based compounds could not be detected in the sample sintered for 1 h at 1500 °C because of very small amount. But when the sample was sintered for 4 h (at 1500 °C), significant amounts of Ni based compounds were formed, as a result some peaks Ni–Si intermetallic could be detected during XRD analysis, whereas other Ni based compounds could not be detected due to small quantities. When the temperature was increased to 1600 °C, the process of decomposition accelerated, hence the amount of TiC_x increased in the system which led to the increase in the peak intensity of TiC_x during XRD analysis.

Thus the sintering of TSC powder was controlled by the two different mechanisms, the interface reactions and the diffusion processes; however, the exact nature of dominating diffusion mechanism, i.e. grain boundary diffusion or lattice diffusion, could not be clearly identified at present. The sintering mechanism was changed to the liquid phase sintering when nickel was added.

3.3. Mechanical properties

Based on the XRD profiles, density data and fine microstructure of the samples sintered at 1500 °C for 1 h, were chosen to test the mechanical properties. TSC sample (96% density) shows Vickers hardness of 2.7 GPa at a load of 5 kg, which was increased to 3.4 GPa for TSC–1Ni sample. The hardness of TSC–1Ni sample was slightly lower than that of the reported value of hot pressed-fully dense material [5]. The flexural strength of TSC–1Ni sample was found to be about 311 ± 22 MPa which was significantly higher than the strength of TSC sample (226 ± 18 MPa). The SEM examination of the fractured surface of TSC–1Ni sample revealed the evidence of ductile fracture (Fig. 11), a characteristic similar to the metals. The fracture toughness of TSC sample was very low (1.8–4.1 MPa $m^{1/2}$) for a/W ratio (where a is the average precrack length and W is the thickness of the beam) of 0.35–0.70, whereas TSC–1Ni sample showed improved toughness (range from 2.8 to 6.4 MPa $m^{1/2}$). The fracture toughness of the fully dense hot pressed TSC (which contains more than 10% of TiC) was reported [33] to vary from 5 to 8.5 MPa $m^{1/2}$ for a/W ratio of 0.35–0.70. Like the hot pressed sample, the microstructure-crack path interaction in the present sample (TSC–1Ni) shows (Fig. 12) the tortuous nature of the crack-path which could be attributed to the crack deflection at the weak interfaces. The crack-bridging and the distortion in the crack path could be seen in the sample (Fig. 12). Since the material synthesised in the present work is of very high purity (i.e., the amount of TiC is negligible), the lower values of hardness, flexural strength and fracture toughness could be possible compared to that of the hot pressed samples reported in the literature.

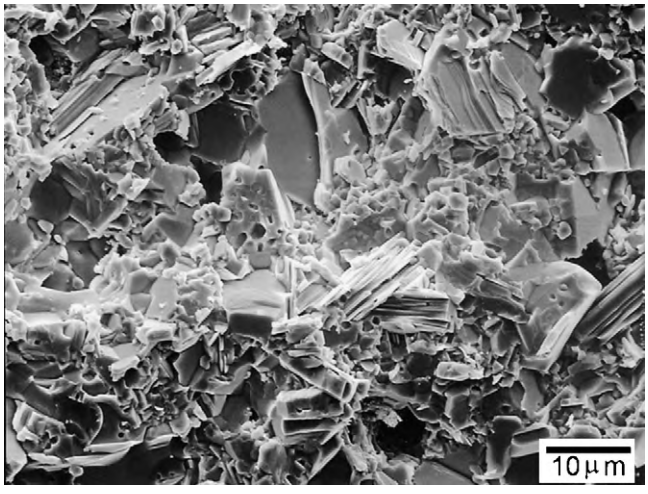

Fig. 11. SEM micrograph of the fractured surface of a TSC–1Ni sample, sintered at 1500 °C for 1 h.

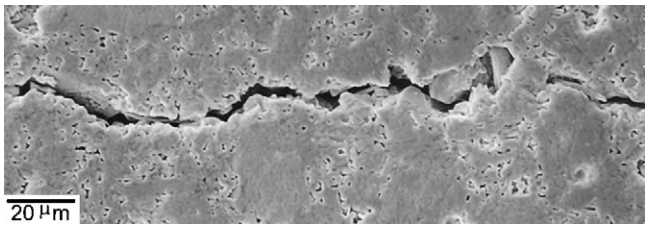

Fig. 12. The crack path propagation of TSC–1Ni sample (sintered at 1500 °C for 1 h), revealing the crack-bridging phenomena.

4. Conclusions

The relative sintered density of 98.5% was achieved using small amount of nickel during pressureless sintering of TSC powder. The activation energies of sintering were determined to be 351 ± 5 and 305 ± 10 kJ/mol for TSC and TSC–1Ni powders, respectively. The sintering was accompanied by the interface reactions and the diffusion of silicon in TSC powder, whereas TSC–1Ni powder exhibited liquid phase sintering behaviour. The bulk TSC–1Ni sample prepared under optimized condition showed good mechanical properties.

Acknowledgement

BBP wishes to acknowledge the Portuguese Foundation of Science and Technology (FCT), program "Compromisso com a Ciência".

Appendix A.

See Table A.1.

Table A.1
Activation energies (A.E.) of diffusions in various systems.

Process	A.E. (kJ/mol)	Ref.
Siliciding of Ti_3SiC_2	156	[34]
Carburization of Ti_3SiC_2	514	[34]
Ti diffusion in Si	198, 173	[35–37]
Si diffusion in α-Ti	105	[38]
Si diffusion in β-Ti	149	[39]
Si diffusion in $TiSi_2$	169	[34]
Ti diffusion in TiC_x	738	[40]
^{14}C diffusion in $TiC_{0.97}$	399	[40,41]
^{14}C diffusion in $TiC_{0.89}$	447	[40,41]
^{14}C diffusion in $TiC_{0.67}$	207	[40]
^{14}C diffusion in $TiC_{0.47}$	464	[40,41]
C diffusion in Si	84, 282	[42,43]
Si diffusion in amorphous C	154	[44]

References

[1] M.W. Barsoum, Porg. Solid State Chem. 28 (2000) 201–281.
[2] J. Wang, Y. Zhou, Ann. Rev. Mater. Res. 39 (2009) 415–443.
[3] M.W. Barsoum, T. Zhen, S.R. Kalidindi, M. Radovic, A. Murugaiah, Nat. Mater. 2 (2003) 107–111.
[4] S Arunajatesan, A.H. Carim, J. Am. Ceram. Soc. 78 (1995) 667–672.
[5] M.W. Barsoum, T. El-Raghy, J. Am. Ceram. Soc. 79 (1996) 1953–1956.
[6] A. Feng, T. Orling, Z.A. Munir, J. Mater. Res. 14 (1999) 925–939.
[7] K. Tang, C. Wang, L. Wu, X. Guo, X. Xu, Y. Huang, Ceram. Int. 28 (2002) 761–765.
[8] Z.F. Zhang, Z.M. Sun, H. Hashimoto, T. Abe, J. Alloys Compd. 352 (2003) 283–289.
[9] Z.M. Sun, S. Yang, H. Hashimoto, J. Alloys Compd. 439 (2007) 321–325.
[10] S. Yang, Z.M. Sun, H. Hashimoto, J. Alloys Compd. 368 (2004) 318–325.
[11] S. Yang, Z.M. Sun, H. Hashimoto, T. Abe, J. Eur. Ceram. Soc. 23 (2003) 3147–3152.
[12] S. Yang, Z.M. Sun, H. Hashimoto, J. Alloys Compd. 368 (2004) 312–317.
[13] N.F. Gao, J.T. Li, D. Zhang, Y. Miyamoto, J. Eur. Ceram. Soc. 22 (2002) 2365–2370.
[14] Y. Khoptiar, I. Gotman, J. Eur. Ceram. Soc. 23 (2003) 47–53.
[15] S. Yang, Z.M. Sun, H. Hashimoto, Mater. Res. Innovat. 7 (2003) 225–230.
[16] D.P. Riley, E.H. Kisi, D. Phelan, J. Eur. Ceram. Soc. 26 (2006) 1051–1058.
[17] C.L. Yeh, Y.G. Shen, J. Alloys Compd. 458 (2008) 286–291.
[18] H. Li, D. Chen, J. Zhou, J.H. Zhao, L.H. He, Mater. Lett. 58 (2004) 1741–1744.
[19] H. Li, L.M. Peng, M. Gong, J.H. Zhao, L.H. He, Zeitschrift für Physikalische Chemie 219 (2005) 1411–1420.
[20] Z.M. Sun, Y. Zou, S. Tada, H. Hashimoto, Scripta Mater. 55 (2006) 1011–1014.
[21] S. Yang, Z.M. Sun, Q. Yang, H. Hashimoto, J. Eur. Ceram. Soc. 27 (2007) 4807–4812.
[22] H.R. Orthner, R. Tomasi, F W.J. Botta, Mater. Sci. Eng. A 336 (2002) 202–208.
[23] W. Sun, D.J. Dcosta, F. Lin, T. El-Raghy, J. Mater. Process. Tech. 127 (2002) 343–351.
[24] J.G. Li, T. Matsuki, R. Watanabe, J. Mater. Sci. 38 (2003) 2661–2666.
[25] A. Murugaiah, A. Souchet, T. El-Raghy, M. Radovic, M. Sundberg, M.W. Barsoum, J. Am. Ceram. Soc. 87 (2004) 550–556.
[26] B.B. Panigrahi, M.C. Chu, A. Balakrishnan, S.J. Cho, J. Mater. Res. 24 (2009) 487–492.
[27] B.B. Panigrahi, Mater. Lett. 61 (2007) 152–155.
[28] G.V. Samsonov, V.I. Yakovlev, Powder Metall. Met. Ceram. 6 (1967) 606–611.
[29] A.K. Khanra, M.M. Godkhindi, Adv. Appl. Ceram. 104 (2005) 273–276.
[30] T. El-Raghy, M.W. Barsoum, J. Am. Ceram. Soc. 82 (1999) 2849–2854.
[31] S.B. Li, G.P. Bei, C.W. Li, M.X. Ai, H.X. Zhai, Y. Zhou, Mater. Sci. Eng. A 441 (2006) 202–205.
[32] L.C. Pathak, S.K. Mishra, P.G. Mukunda, M.M. Godkhindi, D. Bhattacharya, K.L. Chopra, J. Mater. Sci. 29 (1994) 5455–5461.
[33] D. Sarkar, B. Basu, M.C. Chu, S.J. Cho, Ceram. Int. 33 (2007) 789–793.
[34] T. El-Raghy, M.W. Barsoum, J. Appl. Phys. 83 (1998) 112–119.
[35] H. Nakashima, T. Sadoh, H. Kitagawa, K. Hashimoto, Mater. Sci. Forum 143–147 (1994) 761–766.
[36] K. Ishiyama, Y. Taga, A. Ichimiya, Phys. Rev. B 51 (1995) 2380–2386.
[37] S. Hocine, D. Mathiot, Appl. Phys. Lett. 53 (1988) 1269–1271.
[38] J. Raisanen, J. Keinonen, Appl. Phys. Lett. 49 (1986) 773–775.
[39] Y. Iijima, S.Y. Lee, K. Hirano, Philos. Mag. A 68 (1993) 901–914.
[40] S. Sarian, J. Appl. Phys. 40 (1969) 3515–3520.
[41] S. Sarian, J. Appl. Phys. 39 (1968) 3305–3310.
[42] A.K. Tipping, R.C. Newman, Semiconductor Sci. Technol. 2 (1987) 315–317.
[43] R.C. Newman, J. Wakefield, J. Phys. Chem. Solids 19 (1961) 230–234.
[44] E. Vainonen-Ahlgren, T. Ahlgren, L. Khriachtchev, J. Likonen, S. Lehto, J. Keinonen, C.H. Wu, J. Nuclear Mater. 290–293 (2001) 216–219.